UNAMBIGUOUS, HIGH RESOLUTION, AND WIDE SWATH SYNTHETIC APERTURE RADAR IMAGING

Devindran Rajakrishna

Radar Systems and Remote Sensing Laboratory
University of Kansas Center for Research, Inc.
2291 Irving Hill Road, Lawrence, Kansas 66045-2969, USA
785/864-4835 * Fax, 785/864-7789 * graham@rsl.ukans.edu

RSL Technical Report 13130-1

May 1998

Sponsored by:

Air Force Defense Research Sources Program
Culver City CA 90230-6609

Document 97-0880

TABLE OF CONTENTS

LIST OF SYMBOLS

Number	Symbol	Unit	Description
1.	v	m/s	velocity of radar
2.	s	m/s	velocity of object
3.	T	s	observation time of radar
4.	R_s	m	swath width (across-track)
5.	l_x	m	along-track image length
6.	l_y	m	across-track image width
7.	B	Hz	bandwidth of radar system
8.	prf	Hz	pulse repetition frequency
9.	h	m	above-ground height of radar
10.	θ	degrees	tilt angle of radar antenna
11.	L_x	m	along-track aperture length
12.	L_y	m	across-track aperture height
13.	λ	m	radar operating wavelength
14.	f	Hz	radar operating frequency
15.	c	m/s	velocity of light
16.	Δx	m	along-track image resolution
17.	Δy	m	across-track image resolution
18.	D	m	antenna length
19.	R	m	radar-to-target slant range

Number	Symbol	Unit	Description
20.	$\mathbf{r_o}$	m	initial position vector (p.v.) of object
21.	$\mathbf{r_p}$	m	p.v. of object any time t
22.	$\mathbf{r_s}$	m	p.v. of transmitter (Tx) at time t
23.	n	-	particular receiver (Rx) used
24.	$\mathbf{r_r}'$	m	p.v. of Rx with respect to (wrt) Tx
25.	$\mathbf{r_r}$	m	p.v. of Rx wrt object origin
26.	E	V/m	electric (E) field component at Rx
27.	W	-	Tx antenna pattern
28.	Y	m^2	Rx antenna pattern
29.	Z	m^2	complex radar cross section of target
30.	P_t	m^{-2}	propagation from Tx to object
31.	P_r	m^{-2}	propagation from object to Rx
32.	K	V/m	frequency spectrum of radar pulse
33.	k_x	m^{-1}	along-track spatial frequency
34.	k_y	m^{-1}	across-track spatial frequency
35.	k_z	m^{-1}	height direction spatial frequency
36.	k	m^{-1}	wave number
37.	J	V/m	total E-field component response
38.	R_i	V/m	magnitude of E-field for point i
39.	K_i	V/m	E-field at i (with unity rcs)

ABSTRACT

The current performance issues related to a single receiver Synthetic Aperture Radar (SAR) were studied and illustrated. Specifically, the tradeoffs between swath, resolution and ambiguity in both the across-track and along-track directions were considered and documented. To improve upon current performance, it is proposed that the SAR be modeled in a multiple receiver environment. To physically illustrate the current situation and proposed solution, a SAR simulator was constructed using the C programming language. A square image was used to represent a target area. A single receiver SAR environment was developed and the data obtained clearly demonstrated the shortcomings of the present system. Subsequently, a multiple receiver SAR environment was created. The data collected has proven that a multiple receiver SAR produces higher performance with respect to swath width, resolution and ambiguity. Specifically, it has been shown that in a multiple receiver SAR environment, it is now possible to obtain wide swath, high resolution, and unambiguous SAR images within a wide range of pulse repetition frequencies.

1 SYNTHETIC APERTURE RADAR IMAGING

1.1 Overview

Synthetic Aperture Radar (SAR) [1] is a powerful surveillance tool that can perform a multitude of functions in an all-weather day and night situation. In the military area, SAR may be used as a ground surveillance system to monitor troop and equipment activity. In the civilian area, SAR is a popular choice for ocean surveillance and deforestation assessment.

This type of radar employs signal processing techniques to effectively obtain the performance of a long antenna whilst maintaining a relatively short physical one, hence the term "Synthetic Aperture Radar". This technique was developed in response to the need for improvement in radar imaging resolution, especially in the direction of radar flight.

1.2 Current SAR Performance Limitations

There are two critical criteria that a SAR needs to fulfill in order to perform optimally. Firstly, it must be able to map a wide spatial area in order to locate all objects of interest. In addition, it must also be able to exhibit fine resolution in order to specifically identify particular objects on the ground. Unfortunately, these two criteria are not easily achieved at the same time because of a tradeoff that is currently inherent in standard SAR sensors: observations of high spatial resolution are achieved unambiguously only when the swath width of

the observed area is limited. Given that the converse of the previous statement is also true, it is now clear that this limitation could seriously inhibit the ability of a standard SAR sensor to produce unambiguous, wide swath, and high resolution images.

1.3 Ongoing Research

There has been much research performed in this area to attempt to limit the impact of the above restriction. Possible techniques for obtaining wide swath SAR images are presented in [2] and [3]. These references primarily focus on techniques now referred to as Multiple Elevation Beam (MEB) and Multiple Azimuth Beam (MAB). Whilst these techniques are effective, they each possess shortcomings. With MEB SAR, the discontinuous swath in the across-track direction affects the clarity of the imaged area. With MAB SAR, there remains unresolved ambiguities in the doppler direction due to overlap of the sidelobe beams with that of the mainlobe. Yet another technique [4] involving the use of a broader elevation-plane beamwidth only reduces ambiguity in range. Furthermore, the suggested algorithms for this method are computationally intensive and could place a limit on the hardware used. Finally, efficient filtering methods [5] to improve upon the resolution of SAR images have also been offered, but (as they use a variation of the MAB technique) assume that ambiguities have been resolved. In addition, in all the techniques mentioned

above, the theories presented have not been physically illustrated with a SAR imaging simulator.

1.4 Motivation

This thesis deals with the proposal to employ the use of multiple receive apertures in a SAR antenna as a method of removing the swath width - ambiguity tradeoff currently present in a conventional SAR.

With the introduction of these multiple receivers, it now becomes possible to increase the number of samples taken by the SAR over a fixed observation time and thus remove swath width - ambiguity tradeoff. With these additional samples, the SAR may now be (perhaps) able to eliminate ambiguity and observe a wide swath width simultaneously. This is presently not easily achieved in the case of a standard SAR sensor.

1.5 Aim

The aim of this project is to introduce, discuss and physically validate the theory and concepts leading to the development of a Synthetic Aperture Radar model that utilizes the concept of multiple receive apertures and digital beamforming techniques [6,7] to produce unambiguous, wide swath, and high resolution images.

1.6 Current Situation

Figure 1.1 shows the basic geometry of the SAR model. A fully focused airborne SAR traveling at a speed of v will image over a time T a total area of approximately $R_s vT$, where R_s is the ground swath coverage in the across-track direction.

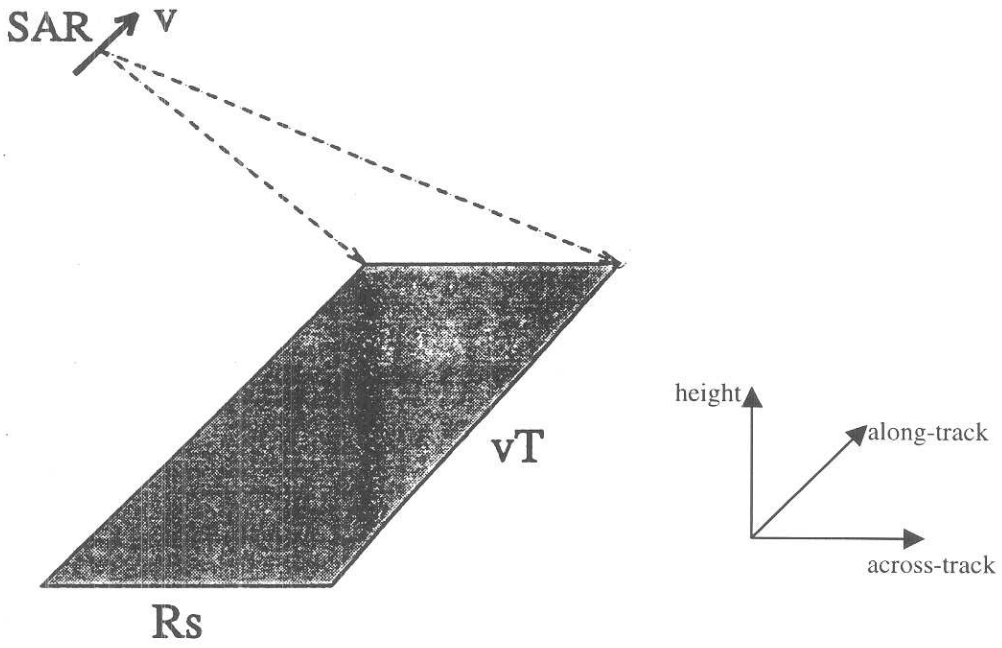

Figure 1.1: Basic Geometry of the SAR Model (Adapted from [8])

We shall say that this imaged area, A, has an along-track length of l_x and an across-track width of l_y. Therefore,

$$A = l_x l_y \approx R_s vT . \qquad (1.1)$$

A standard SAR sensor with a single receiver of bandwidth B will amass complex data at a rate equal to the bandwidth B. If the total observation time is fixed at T seconds, then we can expect this sensor to collect a total of BT independent complex samples over this observation period. With this data, an unambiguous image of up to BT pixels may now be constructed.

The SAR sensor must not illuminate more than BT resolution cells if we wish to avoid ambiguity. Here, a "resolution cell" has a length represented by the SAR's along-track resolution and a width represented by its across-track resolution. If there are more than BT pixels illuminated, then the scattered energy from the extra area will appear in pixels of the imaged area, thus causing ambiguity. We are at liberty to develop a large image of moderate resolution, or a smaller image of high resolution. But in both cases, we remain constrained by the time-bandwidth product so long as we wish to produce an unambiguous image.

To avoid ambiguities, the pulse repetition frequency (prf) has to be carefully chosen. We require a low pulse repetition frequency to avoid range ambiguities. At the same time, a high pulse repetition frequency is required to eliminate ambiguity in the doppler direction. If the SAR antenna beamwidth illuminates more than BT resolution cells over an observation time T, then no value of the prf can be found to produce an unambiguous image.

1.7 The Use of Multiple Receive Apertures

If, however, we were now to implement N receive apertures, each with a coherent receiver, then the total number of independent samples available would increase to NBT. This now enables us to obtain an image with either greater resolution or larger size. As an example, let us consider the implementation of a three receive aperture antenna array. A graphical illustration of this is shown in Figure 1.2. We observe the existence of a low transmit pulse repetition frequency to accommodate a wide swath width. This results in the synthesized aperture being undersampled in the along-track direction. However, the spatially displaced receive apertures now provide the additional samples and, in essence, enable the synthesized receive aperture to now exhibit spatial samples of a SAR with N times the pulse repetition frequency [8].

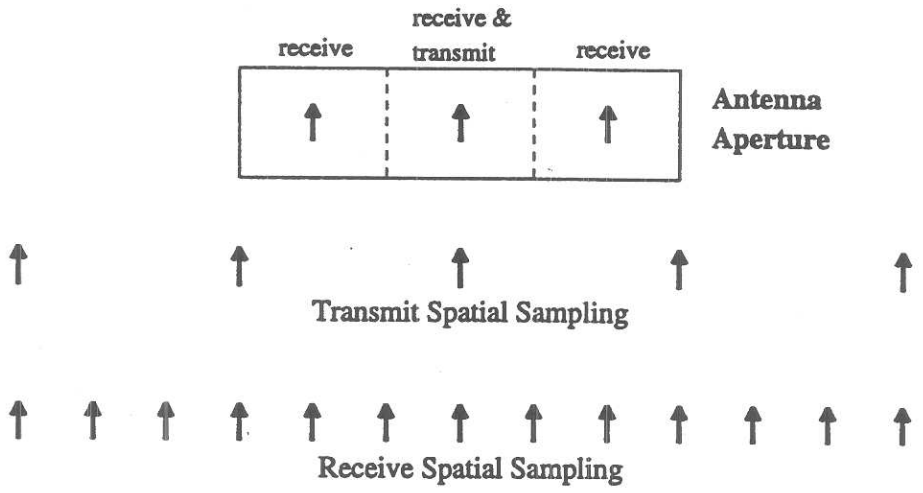

Figure 1.2: SAR Spatial Sampling in Doppler (Reproduced from [8])

Since the single transmit element shares an aperture with the center receive element, we can now say that the along-track illumination pattern of each of the receive elements and the single transmit element are identical and will have a beamwidth three times larger than the original single receive aperture. When added correctly, the azimuthal response of these three sub apertures will be equivalent to that of a single larger receive aperture [8]. This now provides us with a beamwidth narrow enough to eliminate along-track ambiguity.

The three element receiver is essentially implemented as a phased array. Since each element is individually and coherently detected, digital beamforming may now be used in the processing of data. Because each sub aperture possesses a broader beamwidth than a single large aperture of the collective length, a single target may be observed long enough to obtain a fine along-track resolution. At the same time, the coherent adding of the receiver channels will now ensure that there will be a sufficiently narrow beam in the doppler direction to eliminate along-track ambiguities.

1.8 Thesis Structure

This thesis is divided into five chapters. Chapter One contains an overview of Synthetic Aperture Radar and its main uses in imaging. Included here are the critical criteria that typify the SAR and its operation. Also mentioned is a summary of the current and past research in this area as well as their

shortcomings. Following this is a detailed analysis and breakdown of the present situation involving SARs. Detailed explanations are provided into its current workings and limitations in terms of performance. Our proposed solution is also introduced and theoretically explained.

Chapter Two provides the detailed mathematics behind the development of the multiple receive element SAR simulator. A complete derivation is provided here, beginning with the definition of the SAR model in question and thereafter proceeding to the definition and performance of all components of the multi channel SAR systems environment.

Chapter Three deals with the design of a suitable simulation environment for the testing of the multiple receive aperture SAR simulator. With the design parameters obtained, a numerical example is also shown to highlight once again the restrictions imposed by the present system and the possible benefits of the proposed solution. In addition, the calculations are performed in a particular manner in order to prove that the theoretical concept proposed would be appropriate for implementation in both fully and partially focused SAR.

Chapter Four details the results obtained from the simulation and testing of the proposed multiple receive aperture SAR model. A test matrix of fifteen different situations was developed. The first half of this matrix focused on the single receive aperture SAR environment whereas the second half of the matrix represents the transition to a multiple receive aperture environment. Resulting

images for all situations were generated to gauge the effectiveness of the proposed solution in relation to the current situation.

Chapter Five represents the wrap up of this thesis. The conclusion reiterates the current problems and the encouraging results obtained after implementation of our proposed multiple receiver SAR solution. In addition, as the multiple receive aperture SAR simulator has been developed with additional functionality for detection of moving targets, there are thus also several possible recommendations listed pertaining to the future use of this simulator for research into SAR moving target indication (MTI).

2 THE MULTIPLE RECEIVE ELEMENT SAR MODEL

2.1 Radar and Object Positions

Figure 2.1 presents the geometry for the SAR model in question. In the development of this model, we have invoked the flat earth approximation.

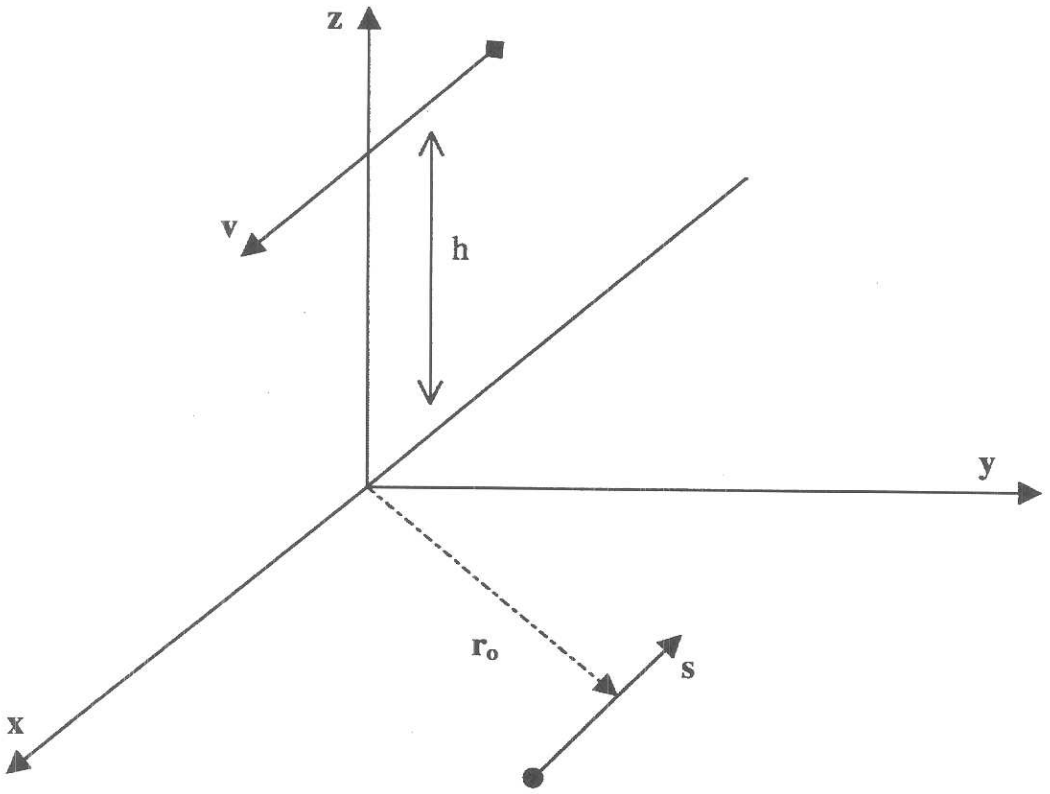

Figure 2.1: Radar and Object Coordinate Geometry

We observe a three-dimensional grid in the **x** (along-track or doppler), **y** (across-track or range), and **z** (height) directions. The radar maintains a height h above the ground. It also travels in the **x** direction with a speed v. Therefore, the velocity vector of the radar may be defined as

$$\vec{v} = v\hat{x}\,. \tag{2.1}$$

We define time t = 0 as the point where the radar is at coordinates {0,0,h}. The initial position vector of an object on the ground can now be defined as

$$\vec{r}_o = a\hat{x} + b\hat{y}\,, \tag{2.2}$$

where a and b are arbitrary scalars.

This object may also have a velocity vector s with components in the **x**, **y** and **z** directions. Thus, the position vector of this object at any time t may be defined as

$$\vec{r}_p = t\vec{s} + \vec{r}_o\,. \tag{2.3}$$

If the object in question is stationary, we would naturally expect its velocity vector to be null. It also follows then that

$$\vec{r}_p = \vec{r}_o\,, \tag{2.4}$$

when t = 0. This is in agreement with our earlier definition of the radar position at time t = 0.

We thus note here that equation (2.4) is always valid when dealing with stationary objects since the velocity vector is null in that case.

2.2 Receiver and Transmitter Positions

Figure 2.2 shows the geometry of the radar antenna with respect to the conventional axes. It is important to note here that the radar antenna is commonly

tilted at an angle to the ground. Thus the coordinate axes of the radar antenna are not identical to the coordinate axes already defined previously for the object. The radar antenna is tilted towards the ground such that the normal out of the plane of the antenna, $\mathbf{z}'$, makes an angle θ with the **z** axis.

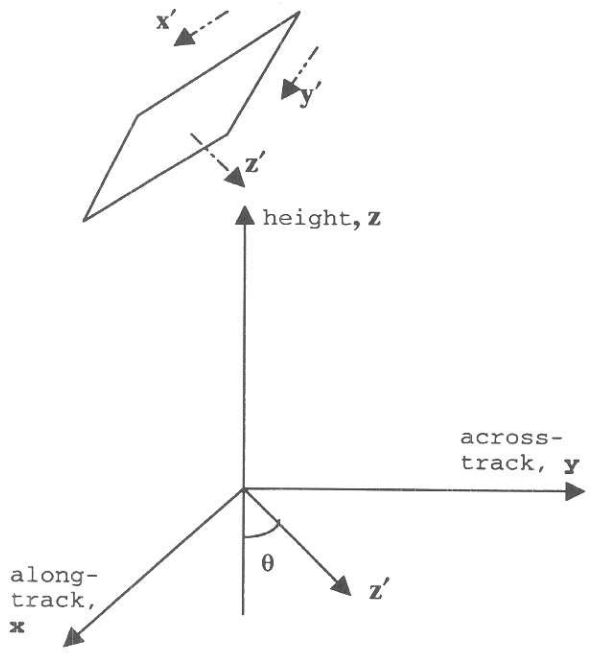

Figure 2.2: Radar Antenna Coordinate Geometry

From the geometry provided in Figure 2.2, the radar antenna coordinate axes can now be determined to be:

$$\hat{x}' = \hat{x}\,, \tag{2.5}$$

$$\hat{y}' = (-\cos\theta)\hat{y} - (\sin\theta)\hat{z}\,, \tag{2.6}$$

and

$$\hat{z}' = (\sin\theta)\hat{y} - (\cos\theta)\hat{z}\,. \tag{2.7}$$

A complete derivation of equations (2.5) through (2.7) is provided in Appendix A.

Figure 2.3 also illustrates the proposed radar antenna receiver and transmitter design. A single transmitter, Tx, is located at the center of the radar antenna. Traditionally, the antenna will possess a single receiver as well. However, we now propose implementing multiple receivers, Rx, within the radar antenna.

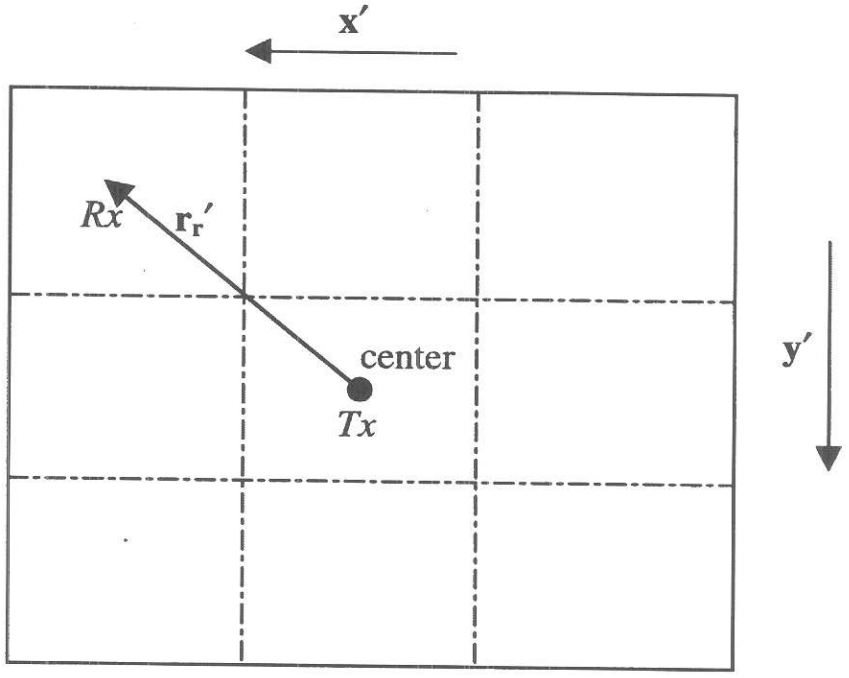

Figure 2.3: Radar Antenna Example Layout

In Figure 2.3, there are now nine receive elements, with the center receive element occupying the same location as the single transmitter.

The position of the radar transmitter can now be defined to be

$$\vec{r}_s = t\vec{v} + h\hat{z}. \tag{2.8}$$

However, based on equation (2.1), we may now rewrite equation (2.8) as

$$\vec{r}_s = vt\hat{x} + h\hat{z}. \tag{2.9}$$

It may also be inferred directly from equations (2.8) and (2.9) that

$$\vec{r}_s = h\hat{z}, \tag{2.10}$$

when $t = 0$.

From Figure 2.3, the position of any radar receiver with respect to the transmitter is defined as

$$\vec{r}_r' = c\hat{x}' + d\hat{y}', \tag{2.11}$$

where c and d are arbitrary scalars.

Finally, the position of any radar receiver with respect to the origin of the object coordinate axes is now

$$\vec{r}_r = \vec{r}_s + \vec{r}_r'. \tag{2.12}$$

We notice here that the nine receive apertures in Figure 2.3 are laid out in a three by three orientation. Firstly, it is important to note that there may be any number of receive apertures in a system. This may be set during the design phase. As the number of receive apertures increases, so will the number of independent samples collected. In addition, the multiple receivers may not necessarily be lined up one against another. In other words, there may also be space placed between

receivers. This allows us to focus specifically on a particularly narrow illumination area. In this instance, careful design will be required to ensure that the range and doppler ambiguities do not coincide within the antenna illumination patterns of the SAR. We should also recognize that it is possible to design the apertures in any orientation as well. For example, the design in Figure 2.3 may also be represented in a nine by one or one by nine manner. The decision on the orientation of the apertures will depend on the selection of the pulse repetition frequency. A choice of a high pulse repetition frequency would require us to line the apertures up in the across-track direction so as to eliminate ambiguity in the direction of range. Similarly, a low pulse repetition frequency selection will require that the apertures be lined up in the along-track direction so as to eliminate ambiguity in the doppler direction.

2.3 Receiver Electric Field Component Response

The complex component response from the electric field at each receive aperture of this multiple channel SAR model can be defined as

$$E_n(\vec{r}_r^{\,n}, f, t) = W \times Y \times Z \times P_t \times P_r \times K . \qquad (2.13)$$

Here, W is the transmitter antenna pattern,

Y is the receiver antenna pattern,

Z is the complex radar cross section of the object,

P_t is the mathematical representation of the propagation from the transmitter to the object,

P_r is the mathematical representation of the propagation from the object to the receiver,

K is the spectrum of the transmitted radar pulse,

and n is the particular receive aperture used.

We notice straightaway that equation (2.13) is, in essence, a complex form of the Radar Range Equation [9]. It is also important to see at this point that this multiple channel SAR model provides an electric field component output response for every step of time, frequency, and receive aperture position. The multiple receive apertures will provide an extra degree of freedom that now enable us to obtain a larger number of independent samples, thus removing the restriction imposed by the time-bandwidth product.

2.4 Antenna Pattern Definitions

Figure 2.4 depicts the layout of a single receiver (or transmitter) aperture for the multi channel SAR model.

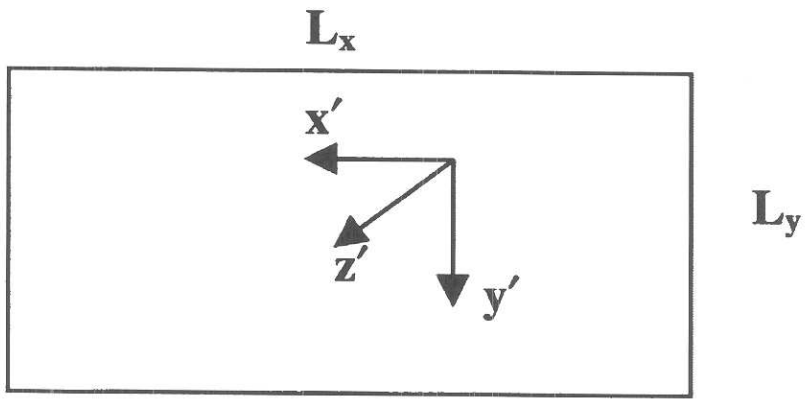

Figure 2.4: Radar Antenna Single Aperture Layout

The height of the aperture in the **y′** (or across-track) direction is given as L_y and the length of the aperture in the **x′** (or along-track) direction is given as L_x.

We can see here that the single transmit aperture is of the same size as each receive aperture. The single transmitter is also located at the center of the array. Whereas the conventional approach has been to design a single transmitter-receiver unit, we now instead propose implementing an antenna array that maintains a single transmitter but possesses multiple receive elements oriented in a chosen manner.

Once again, we note that the **x′** axis corresponds to the along-track direction and the projection of the **y′** axis corresponds to the across—track

direction. Finally, this entire antenna is tilted to face the ground in such a manner that its normal, $\mathbf{z}'$, will make an angle of θ with the $\mathbf{z}$ direction of the conventional axes.

The transmitter antenna pattern of the radar antenna may be next defined as

$$W = \sqrt{\frac{4\pi}{\lambda^2} L_x L_y}\, \sin\left[\frac{k_x L_x}{2}\right] \sin\left[\frac{k_y L_y}{2}\right]. \tag{2.14}$$

Here, the operating wavelength λ is defined as

$$\lambda = \frac{c}{f}, \tag{2.15}$$

where c is the speed of light and f is the operating frequency of the radar.

In addition, k_x is the $\mathbf{x}$ component of the spatial frequency, and is defined as

$$k_x = k\left[\hat{x}' \bullet \frac{\vec{r}_p - \vec{r}_s}{\left|\vec{r}_p - \vec{r}_s\right|}\right]. \tag{2.16}$$

Here, k is the wave number and is defined as

$$k = \frac{2\pi}{\lambda}. \tag{2.17}$$

Similarly, k_y is the $\mathbf{y}$ component of the spatial frequency and is defined as

$$k_y = k\left[\hat{y}' \bullet \frac{\vec{r}_p - \vec{r}_s}{\left|\vec{r}_p - \vec{r}_s\right|}\right]. \tag{2.18}$$

We can confirm here that the transmitter antenna pattern as defined in equation (2.14) is a dimensionless quantity. This is consistent with the fact that W is simply a scaling factor.

We also can state here that

$$k_x^{\,2} + k_y^{\,2} + k_z^{\,2} = k^2, \tag{2.19}$$

or, equivalently,

$$k = \sqrt{k_x^{\,2} + k_y^{\,2} + k_z^{\,2}}\,. \tag{2.20}$$

Similarly, the antenna pattern of the receiver may next be defined as

$$Y = \sqrt{L_x L_y}\,\sin\left[\frac{k_x L_x}{2}\right]\sin\left[\frac{k_y L_y}{2}\right]. \tag{2.21}$$

From equations (2.14) and (2.21), we can derive the ratio of the transmitter antenna pattern to the receiver antenna pattern to be

$$\frac{W}{Y} = \sqrt{\frac{4\pi}{\lambda^2}}\,. \tag{2.22}$$

This is analogous with the theoretical result that was derived in [10].

2.5 Complex Radar Cross Section

Every object on the ground will possess a unique radar cross section due to its position vector with respect to the origin. This complex value, Z, is such that

$$Z = \sqrt{\sigma} e^{j\phi}. \tag{2.23}$$

Here, σ is commonly referred to as the radar cross section (rcs) and influences the amount of radar electromagnetic energy scattered by an object on the ground, and ϕ is the random phase representation between the object on the ground and the SAR.

2.6 Pulse Propagation

The pulse emitted from the transmitter of the SAR travels towards the ground as an electromagnetic wave. From [11], we may define that the propagation of an electromagnetic wave in the direction of any position vector **r** conforms to the following wave equation:

$$P = \frac{\exp(jk|\vec{r}| - j\omega t)}{|\vec{r}|}, \tag{2.24}$$

where k is the wave number,

ω is the angular frequency,

and t is the time instant.

Since the term ωt in equation (2.24) is independent of position in space, it is more common for equation (2.24) to be expressed as

$$P = \frac{\exp(jk\,|\,\vec{r}\,|)}{|\,\vec{r}\,|}. \qquad (2.25)$$

We are now able to adapt equation (2.25) for our purposes in designing the multi channel SAR model. We should first take note that in our case, it is necessary to monitor the electromagnetic wave as it travels from the transmitter to the target as well as when it returns from the target to the receiver. Therefore, we are required to define two electromagnetic wave propagation equations.

In the situation where the electromagnetic wave travels from the transmitter to the target, the pulse propagation equation may be defined as

$$P_t = \frac{\exp(jkm)}{m}, \qquad (2.26)$$

where

$$m = |\,\vec{r}_p - \vec{r}_s\,|. \qquad (2.27)$$

Similarly, we may next proceed to define the pulse propagation equation from the target on the ground to the receiver on the SAR to be

$$P_r = \frac{\exp(jkq)}{q}, \qquad (2.28)$$

where

$$q = |\,\vec{r}_r^{\,n} - \vec{r}_p\,|. \qquad (2.29)$$

It is important to note here that both P_t and P_r are complex quantities. This then results in the final electric field component output response in equation (2.13) turning out to be a complex quantity as well.

2.7 Pulse Spectrum

Figure 2.5 shows the pulse g(t) used as the transmitted signal from the radar. This figure was reproduced from [12].

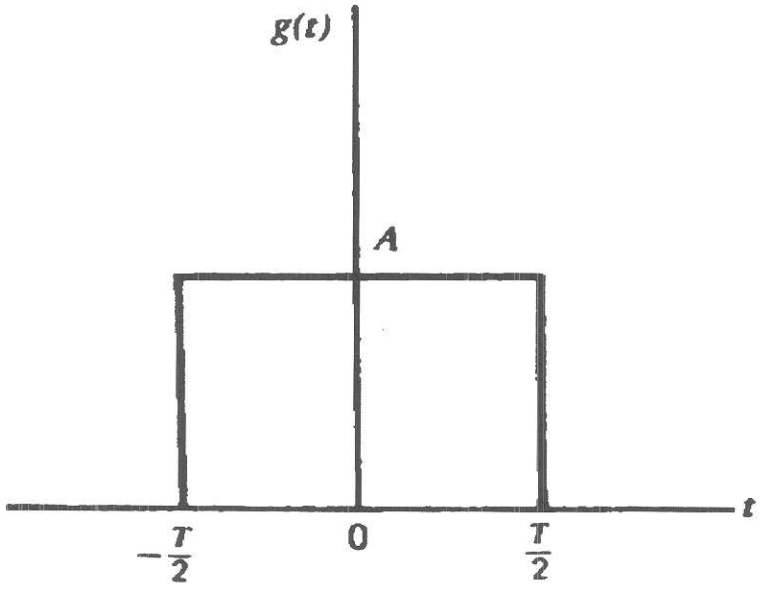

Figure 2.5: Transmitted Radar Pulse

In our situation, we have normalized g(t) such that it provides us with unity area. This now requires us to specify the following:

$$A \times T = 1. \tag{2.30}$$

This constraint thus leads us to

$$A = \frac{1}{T}. \tag{2.31}$$

We may now define g(t) as follows:

$$g(t) = A \times \text{rect}\left[\frac{t}{T}\right], \tag{2.32}$$

where rect(t) is the rectangular function of unit amplitude and duration centered at $t = 0$.

The spectrum of this pulse g(t) may be obtained by computing its Fourier Transform. By definition,

$$G(f) = \Im\{g(t)\} = A\int_{-T/2}^{T/2} \exp(-j2\pi ft)dt. \tag{2.33}$$

Evaluating this integral, we can arrive at

$$G(f) = AT\left[\frac{\sin(\pi fT)}{\pi fT}\right]. \tag{2.34}$$

Since the spectrum we expect to obtain will be complex, it is commonly viewed, as shown in Figure 2.6, in terms of the absolute value of G(f) [12].

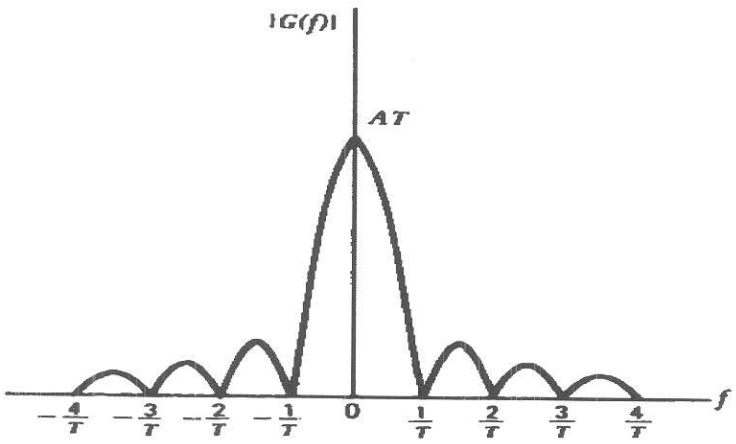

Figure 2.6: Amplitude Spectrum of Rectangular Pulse

We should also note that in our case, the SAR utilizes an operating frequency that is non-zero. Thus the spectrum that we expect to obtain would not be centered at zero frequency but, instead, about the operating frequency. Specifically, equation (2.34) should, in our situation, now be more appropriately written down as

$$G(f) = AT\left[\frac{\sin(\pi(f - f_c)T)}{\pi(f - f_c)T}\right], \qquad (2.35)$$

where f_c is the operating frequency that the radar is currently utilizing.

Based on the provided operating (center) frequency, frequency sampling is performed in steps of the pulse repetition frequency. Time sampling is also performed in steps of the reciprocal of the pulse repetition frequency.

2.8 Matched Filters in Target Detection

The SAR model developed thus far is able to produce an output response at each receive aperture of the radar antenna for every time and frequency step. A method now needs to be developed to perform target detection. We employ the concept of a matched filter to perform this function.

As explained in [10], a matched filter is a filter whose transfer function is determined by a certain signal in a way that will result in the maximum attainable signal-to-noise ratio (SNR) at the output of the filter when both the signal and white noise are passed through it.

Let us consider a signal s(t) that has a Fourier Transform S(ω). Additive white noise of power spectral density $N_0/2$ is also present and this composite signal is then passed through a linear filter with a transfer function (in the frequency domain) of H(ω). The SNR equation governing this system may now be defined to be

$$SNR = \frac{\left| \int_{-\infty}^{\infty} H(\omega)S(\omega)d(\omega) \right|^2}{\pi N_0 \int_{-\infty}^{\infty} |H(\omega)|^2 \, d(\omega)}. \qquad (2.36)$$

We next invoke Schwarz's Inequality which states that for any two complex signals H(ω) and S(ω),

$$\left| \int_{-\infty}^{\infty} H(\omega)S(\omega)d(\omega) \right|^2 \leq \int_{-\infty}^{\infty} |H(\omega)|^2 \, d(\omega) \int_{-\infty}^{\infty} |S(\omega)|^2 \, d(\omega).$$

(2.37)

Applying equation (2.37) to equation (2.36), we see that in order for the SNR to be maximum,

$$H(\omega) = bS^*(\omega). \tag{2.38}$$

Here, $S^*(\omega)$ is the complex conjugate of $S(\omega)$ whereas b may be any arbitrary constant. Normally, we say that

$$b = 1, \tag{2.39}$$

and this therefore reduces equation (2.38) to

$$H(\omega) = S^*(\omega). \tag{2.40}$$

This concept will now be adapted to our new multiple aperture SAR model. Consider an imaged area illuminated by the SAR. If we assume that this imaged area is square and has 256 pixels in each direction, then there will be a total of 65536 pixels in this image. The sum of all responses from this area may be defined to be

$$J(\vec{r}_r^{\,n}, f, t) = \sum_{i=1}^{i=65536} E_i(\vec{r}_r^{\,n}, f, t). \tag{2.41}$$

Here, E_i is defined as given in equation (2.13). Following this, we would like to match this summed response with a particular point on the ground to obtain an

output response for that point. Here, the output response for any point (pixel) will be defined as

$$R_i = \left| J(\vec{r}_r^{\,n}, f, t) \bullet K_i(\vec{r}_r^{\,n}, f, t) \right|, \tag{2.42}$$

where i now ranges from one to 65536 and K_i is such that

$$K_i(\vec{r}_r^{\,n}, f, t) = E_i'^{*}(\vec{r}_r^{\,n}, f, t). \tag{2.43}$$

As we wish for all our matched filter scattering coefficient component returns to be normalized, the scattering coefficient Z that contributes towards E'_i will now have a unity value, thus distinguishing E_i from E_i'. Therefore, for E_i',

$$Z = 1. \tag{2.44}$$

2.9 Summary

Finally, we have developed a multiple receive element Synthetic Aperture Radar model. This model possesses receivers that are able to detect the returned signal scatter energy at every step of time, frequency, and receive aperture position. What we have developed here, is, in essence, a model that obtains and stores data samples in a three-dimensional storage array of time, frequency and receive aperture position. Following this, we constructed a matched filter that performs the function of target detection.

It is appropriate now to next attempt to set up a suitable simulation environment for our model.

3 DESIGN ENVIRONMENT

3.1 Parameter Design

Given that the SAR has an operating wavelength λ, its along-track resolution can be determined from [9] to be

$$\Delta x = \frac{\lambda R}{2vT}. \tag{3.1}$$

Since the slant range R is defined as

$$R = \frac{h}{\cos\theta}, \tag{3.2}$$

equation (3.1) may now be written as

$$\Delta x = \frac{\lambda h}{2vT\cos\theta}. \tag{3.3}$$

Similarly, the across-track resolution of the SAR may also be found from [9] to be

$$\Delta y = \frac{c}{2B\sin\theta}. \tag{3.4}$$

If we let each pixel be square, then

$$\Delta x = \Delta y. \tag{3.5}$$

Subsequently, by equating and rearranging terms in equations (3.3) and (3.4), we can thus arrive at

$$\frac{B}{T} = \frac{cv\cot\theta}{h\lambda}. \tag{3.6}$$

Making our tilt (or grazing) angle 45°, then from [13] we know that

$$\cot\theta \approx 1, \tag{3.7}$$

we can now further simplify the time-bandwidth ratio in equation (3.6) to be

$$\frac{B}{T} = \frac{vf}{h}. \tag{3.8}$$

Based on design suggestions from [14] and values from typical low earth orbit (LEO) radar applications, we set the following parameters:

$$\text{Radar Height: } h = 183\text{km}, \tag{3.9}$$

$$\text{Radar Speed: } v = 7.8\text{km/s}, \tag{3.10}$$

$$\text{Radar Frequency: } f = 10\text{GHz}, \tag{3.11}$$

and

$$\text{Tilt Angle: } \theta = 45°. \tag{3.12}$$

Using the above values, we can next numerically determine the time-bandwidth ratio in equation (3.8) to be

$$\frac{B}{T} = 4.26\times10^{8}\,\text{s}^{-2}. \tag{3.13}$$

We select a square image containing 256 pixels in both length and width. If we wish to reconstruct the image unambiguously with nine receive apertures, then

$$9BT \geq 256\times256 = 65536. \tag{3.14}$$

This implies that

$$BT \geq 7281. \tag{3.15}$$

Since equation (3.15) merely stipulates a lower bound for the time-bandwidth product, we are able to specify a higher value as well. Let us now say that

$$BT = 10650 . \tag{3.16}$$

Solving equations (3.13) and (3.16) simultaneously, we can determine that

$$B = 2.13\text{MHz} , \tag{3.17}$$

and also that

$$T = 5\text{ms} . \tag{3.18}$$

With these values obtained we can confirm that

$$\Delta x \approx \Delta y \approx 100\text{m} . \tag{3.19}$$

This is now in accordance with equation (3.5).

To eliminate range ambiguities, we can determine from [9] that

$$f_{prf} \leq \frac{c}{2l_y \sin\theta} . \tag{3.20}$$

To eliminate doppler ambiguities, however, we also require from [9] that

$$f_{prf} \geq \frac{2vl_x}{\lambda R} . \tag{3.21}$$

Equations (3.20) and (3.21) clearly illustrate once again the current difficulty faced in reducing ambiguity in both the range and doppler directions.

Rearranging (3.20) and (3.21), we can arrive at

$$l_y \le \frac{c}{2f_{prf}\sin\theta}, \tag{3.22}$$

and

$$l_x \le \frac{f_{prf}\lambda R}{2v}. \tag{3.23}$$

The maximum area may now be determined by setting the values of l_x and l_y to their individual maximum values. Therefore, the maximum area may be found by taking the product of equations (3.22) and (3.23) at the maximum values of l_x and l_y. Specifically,

$$l_x l_y = \frac{c\lambda R}{4v\sin\theta}. \tag{3.24}$$

From this, as well as from (3.1) and (3.4), we can find that

$$\frac{l_x l_y}{\Delta x \Delta y} = \frac{c\lambda R}{4v\sin\theta}\frac{2vT}{\lambda R}\frac{2B\sin\theta}{c} = BT. \tag{3.25}$$

This proves that we require at least BT independent time-bandwidth data samples in order to generate an unambiguous image containing BT pixels. Therefore, the use of BT data samples to generate more than BT image pixels will cause ambiguity.

Replacing (3.24) with its numerical values,

$$l_x l_y = 105.6\times10^6\,m^2. \tag{3.26}$$

Since the image is square,

$$l_x \approx l_y \approx 10.27km. \tag{3.27}$$

In our proposed solution design, we now specify the presence of nine receive apertures instead of just one. Therefore, we now expect our maximum area to be nine times larger. Given that the resolution in both the range and doppler directions is approximately 100 m, we may now set the pixel length in both range and doppler directions to be, say, 105 m. Therefore, the new image length and width is now

$$l_x \approx l_y \approx 26.88\text{km}. \tag{3.28}$$

Finally, we are now able to return to equation (3.20) and calculate that in order to eliminate range ambiguities,

$$f_{prf} \leq 7891\text{Hz}. \tag{3.29}$$

Once again, as equation (3.29) is merely an upper bound, we can specify that in order to eliminate range ambiguities,

$$f_{prf} = 7\text{kHz}. \tag{3.30}$$

Similarly, we are now also able to return to equation (3.21) and calculate that in order to eliminate doppler ambiguities,

$$f_{prf} \geq 54009\text{Hz}. \tag{3.31}$$

As equation (3.31) also stipulates a lower bound, we can next say that in order to eliminate doppler ambiguities,

$$f_{prf} = 60\text{kHz}. \tag{3.32}$$

From [9], the along-track aperture length can be determined to be

$$L_x \leq \frac{\lambda h}{l_x \cos\theta} \approx 29\text{cm}. \tag{3.33}$$

Similarly, the across-track aperture height may now be theoretically found to be

$$L_y \leq \frac{\lambda h}{l_y \cos^2\theta} \approx 41\text{cm}. \tag{3.34}$$

Using these upper bounds, we find the values of L_x and L_y such that the nearest point of ambiguity in both the range and doppler directions lies within the location of the first null of the radar antenna pattern. With this method, we determine the aperture length and height to be, respectively,

$$L_x = 25.5\text{cm}, \tag{3.35}$$

and also that

$$L_y = 37.1\text{cm}. \tag{3.36}$$

This concludes the parameter design phase of the simulation. At this point, we have all necessary design parameters to simulate several different situations.

We notice that, as expected, there are conflicting requirements for the choice of a single radar pulse repetition frequency. We are required to select a value of 60 kHz for the pulse repetition frequency if we wish to eliminate ambiguities in the doppler direction. But, we are also required to select a value of 7 kHz for the pulse repetition frequency if we wish to eliminate ambiguities in

range. This conflicting dependency on the pulse repetition frequency is the problem that we anticipate the multiple receive aperture SAR model to be able to resolve.

3.2 A Numerical Example

With the values obtained, it is now appropriate to develop a numerical example to physically illustrate the present problem and the proposed solution.

It should be noted here that the design methodology provided in the previous section centers on a radar with apertures that are not fully focused, whereas in reality the SAR is often operated with fully focused apertures. This was done only to reduce computation time in the simulation. The problem of obtaining wide swath, unambiguous, and high resolution radar images remains the same, regardless of the type of aperture used. To prove its validity, the following numerical example will use the derived values to illustrate the problem in the case of a fully focused SAR.

In the case of a fully focused SAR, the along-track resolution is defined as

$$\Delta x = \frac{D}{2}, \tag{3.37}$$

where D is the length of the antenna.

Using the value for D found in (3.35) we can say that

$$\Delta x = 0.1275\text{m}. \tag{3.38}$$

Based next on the assumption of square pixels,

$$\Delta y = \Delta x = 0.1275\text{m}. \tag{3.39}$$

Returning to equation (3.4), we can find the bandwidth to be

$$B = 1.67\times10^{9}\,\text{Hz}. \tag{3.40}$$

Similarly, we may next return to equation (3.1) and determine the new observation time to be

$$T = 3.9\text{s}. \tag{3.41}$$

We can see now that a fully focused SAR operating in our defined environment would actually have a bandwidth of 1.67 GHz and a (longer) observation time of 3.9 s. This will only result in a larger time-bandwidth product than that calculated earlier. The qualitative treatment of the problem from this point on remains the same whether one is dealing with a partially focused aperture or a fully focused one.

Assuming the physical aperture length of 25.5 cm, equation (3.21) will require that in order to eliminate doppler ambiguities,

$$f_{prf} \geq 61176\text{Hz}. \tag{3.42}$$

However, since the maximum unambiguous swath width is defined as

$$R_s = \frac{c}{2f_{prf}\sin\theta}, \tag{3.43}$$

we can see that this choice of pulse repetition frequency would seriously limit the unambiguous swath width to be

$$R_s \approx 3500\text{m}. \tag{3.44}$$

On the other hand, we note that the approximate image area may be determined to be

$$A = R_s vT = 1.05\times10^8\,\text{m}^2. \tag{3.45}$$

Since we also know that

$$\frac{A}{\Delta x \Delta y} \le BT, \tag{3.46}$$

we can determine the maximum unambiguous swath width to be

$$R_s \approx 3500\text{m}. \tag{3.47}$$

It is clear now that we have arrived at the same value of maximum unambiguous swath width using two different approaches. We can now see that it is possible to obtain more time-bandwidth samples by simply increasing the number of antenna elements. If we now had N elements, the total number of time bandwidth samples would now have increased by a factor of N to NBT.

Let us now specify a new swath width requirement of three times the value found in equations (3.44) and (3.47). That is, we now want the swath width to be

$$R_s = 10500\text{m}. \tag{3.48}$$

To eliminate range ambiguity at this new swath width, equation (3.20) will require that the new pulse repetition frequency be reduced by a factor of three. Specifically, we now require

$$f_{prf} \leq 20203\text{Hz}. \tag{3.49}$$

Obviously, this value of pulse repetition frequency does not agree with that defined earlier in equation (3.42), and will cause ambiguity in the doppler direction unless the antenna length is altered. Now, to satisfy equation (3.49), we require that the new antenna length be

$$L_x = 25.5\text{cm} \times 3 = 76.5\text{cm}. \tag{3.50}$$

Finally, returning to equation (3.37), this new aperture length would result in degradation of the along-track resolution. Now,

$$\Delta x = 0.1275\text{m} \times 3 = 0.3825\text{m}. \tag{3.51}$$

It is clear that we have now traded swath width for resolution. This is the current problem we face.

If, however, we instead implemented the receive antenna as three individual apertures each of length 25.5 cm, then the number of independent samples increases by three times to 3BT instead of just BT. More importantly, we can see from equations (3.37) and (3.43) that we can now achieve the enlarged swath width of 10500 m whilst maintaining the (original) superior resolution of 0.1275 m because we do not alter the physical length of each aperture. Rather, we have instead employed the use of multiple receive apertures to provide us this increase in overall antenna length.

Because the transmit antenna aperture possesses the same size as the center receive antenna aperture, the illumination patterns in the along-track

direction of the single transmit aperture and the three receive apertures are identical. In addition, each is also three times as broad as that of the original enlarged aperture of length 76.5 cm. From this broader beamwidth of each sub aperture, a single target can be observed long enough to achieve a fine along-track resolution. At the same time, this beamwidth is narrow enough to attenuate ambiguities in the along-track direction.

From this, it is evident that the use of multiple receive apertures has now allowed us to potentially obtain wide swath, high resolution, and unambiguous radar images. It is now an appropriate time to move towards a computer simulation environment and put our proposed theoretical solution to a practical test in order to determine how effective this design is.

3.3 Test Matrix

Following the completion of the parameter design, a test matrix was developed to list the situations to be addressed. This test matrix is listed as Table 3.1 and shows the different input parameters necessary to attain a particular test environment.

Situation	f_{prf} (kHz)	L_x (cm)	L_y (cm)	Apertures (N)	NBT
1	7	25.5	37.1	1	10650
2	7	25.5 * 9	37.1	1	10650
3	60	25.5	37.1	1	10650
4	60	25.5	37.1 * 9	1	10650
5	20.5	25.5	37.1	1	10650
6	20.5	25.5 * 3	37.1	1	10650
7	20.5	25.5	37.1 * 3	1	10650
8	20.5	25.5 * 3	37.1 * 3	1	10650
9	20.5	25.5 by 3	37.1	3	31950
10	20.5	25.5	37.1 by 3	3	31950
11	7	25.5 by 3	37.1 by 3	9	95850
12	7	25.5 by 9	37.1	9	95850
13	60	25.5 by 3	37.1 by 3	9	95850
14	60	25.5	37.1 by 9	9	95850
15	20.5	25.5 by 3	37.1 by 3	9	95850

Table 3.1: Test Matrix for Simulation

As is evident, the first eight situations in this test matrix will reflect the problems present in a single receive aperture SAR environment. The pulse repetition frequency and aperture size will be varied to test a variety of situations with the intention of proving that, whilst it is possible to obtain an image that has

high resolution, wide swath, or low ambiguity, it is not presently possible to have all these traits present in a single image.

In the single receive aperture SAR environment, the physical length and height of the receive aperture is altered to reflect the particular test situation. For example, in Situation 8, the physical aperture length and height is three times as large because the pulse repetition frequency in that instance is less than each extreme by a factor of three. There will be further analysis of each test situation in the following section.

The final seven situations will represent the transition to a considerably more efficient multiple receive aperture SAR environment. Here, the pulse repetition frequency will be varied together with the number of apertures with the intention of obtaining a single image that possesses wide swath, high resolution and low ambiguity.

In the multiple receive aperture SAR environment, we notice that there is no longer a physical change in the size of each aperture. All receive apertures (as well as the single transmit aperture) are of the same size. In the multiple receive aperture SAR environment, several of these receive apertures are placed in a suitable orientation depending on the test situation. For example, in Situation 12, there are nine receive apertures placed in the along-track direction due to the presence of a pulse repetition frequency that only eliminates ambiguity in the

across-track direction. Once again, further analysis of each situation will provided in the following section.

The pulse repetition frequency (f_{prf}) is varied between three values. A value of 60 kHz reflects a situation in which doppler ambiguities will be eliminated. A value of 7 kHz reflects the situation where we wish for range ambiguities to be eliminated. A value of 20.5 kHz was also chosen as it is the geometric mean of the other two test frequencies. This would represent a position of "compromise" between the complete elimination of range and doppler ambiguities in the test environment.

3.4 Test Image

Figure 3.1 shows the test image used for the simulation. This picture was obtained from the KUIM Image Processing System. More details on this system are provided in the next section. This image has (for decades) been an extremely popular choice of input in image processing research. It is understood that this image was first used by researchers in the 1970s and has since become a de facto standard for performance comparisons. The image consists of 65536 pixels oriented in a 256 by 256 manner. The intensity of each pixel ranges from zero (pure black) to 255 (pure white). The along-track direction would be equivalent to viewing this image from east to west (or left to right) and the across-track direction would be equivalent to viewing this image from north to south (or top to bottom).

The intensity of each pixel represents the magnitude of the object radar cross section at each point on the ground. In addition, a random number generator was introduced to implement the random phase component of each point on the ground.

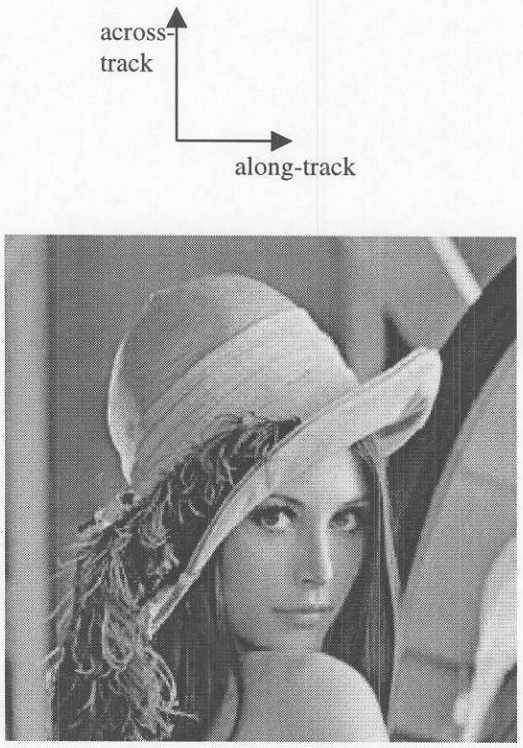

Figure 3.1: Test Image used as Target Area

3.5 Coding of the Multiple Receive Aperture SAR Simulator

The code for this entire project was written using the C programming language [15-16]. There were several reasons for the choice of this language. Firstly, it is an extremely versatile language that is very commonly used in software engineering these days. Hence, they are many qualified people who would be able to read, execute and amend this program as necessary.

Secondly, whilst it was felt that procedural programming would suit this project more than an object oriented style, future changes to the functionality and performance specifications of the program may invariably require a switch towards object orientation. Having a software program already written in C would subsequently make the transition to a C++ environment a relatively painless process.

Thirdly, all C (and C++) code can be implemented as Matlab functions. Matlab is an extremely popular software tool that can be easily used for mathematical and scientific calculations. Being able to port functions of code over to Matlab for verification before implementation in a global framework is a useful aid.

Finally, it was necessary to select an image processing program for processes like image display and pixel intensity rescaling. The package chosen was the KUIM Image Processing System, developed by Prof. John Gauch of the University of Kansas. This entire package is written in a C and C++ environment.

Several chunks of code from KUIM have been adapted for use in the development of software for the multiple receive aperture SAR simulator. An early decision was thus made to maintain a common language throughout the program.

3.6 Graphical Example using the Ambiguity Function

An effective method of presenting a graphical illustration of the problem and proposed concept is to employ the use of the ambiguity function in a radar imaging environment. As stated in [10], the ambiguity function is defined as the absolute value of the envelope of the output of a matched filter when the input to the filter is a doppler-shifted version of the original signal, to which the filter is matched.

Figure 3.2 shows the target area designed. We observe the presence of a single white spot (of intensity 255) in the center of the image. This indicates the presence of a single object at that point. Elsewhere, the presence of pure black pixels (of intensity zero) simply indicates that no object exists at any other point within the imaged area. This designed target area will be used to illustrate the conceptual idea supporting our solution.

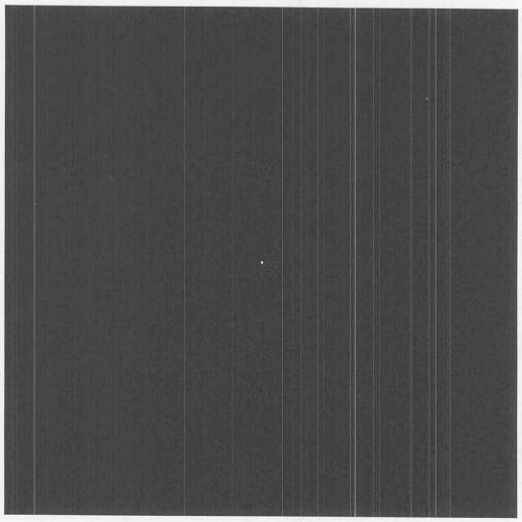

Figure 3.2: Ambiguity Function Test Input

Here, we specify the pulse repetition frequency to be 20.5 kHz. In addition, we also set the along-track length and across-track height of the antenna aperture(s) to be 25.5 cm and 37.1 cm respectively. In the single receiver SAR environment, we can predict that our resultant receiver image will be ambiguous.

Figure 3.3 shows the results obtained in a single receiver SAR test environment. With a prf of 20.5 kHz, we expect an ambiguity factor of three in both range and doppler directions of the resultant SAR image. We notice that in addition to accurately identifying the test point in the center of the image, our single receiver SAR simulator has also falsely detected the presence of several other objects within the test area. It is clear (from Figure 3.2) that these objects do not really exist.

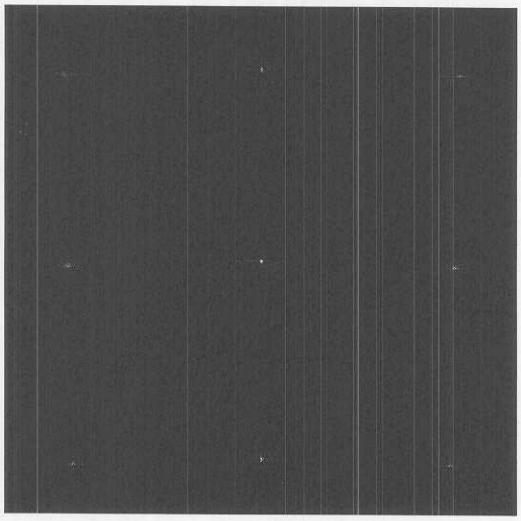

Figure 3.3: Single Receiver Ambiguity Function Test Result

The single receiver SAR simulator has been unable to generate sufficient independent data samples and cannot resolve ambiguities in both its along-track and across-track directions. This has resulted (from Figure 3.3) in a false detection of targets. This current situation is, clearly, unsatisfactory.

The situation can be remedied with the introduction of multiple receivers to the SAR simulator. Since we are faced with an ambiguity factor of three in both directions, we now introduce nine receivers designed in a three by three format, similar to that shown in Figure 2.3. We anticipate that this measure will result in the collection of nine times as many independent data samples. Consequently, this will be sufficient to eliminate ambiguity in both range and doppler directions. Maintaining all previous simulation parameters in a nine

receive aperture SAR environment, we now obtain the results shown in Figure 3.4.

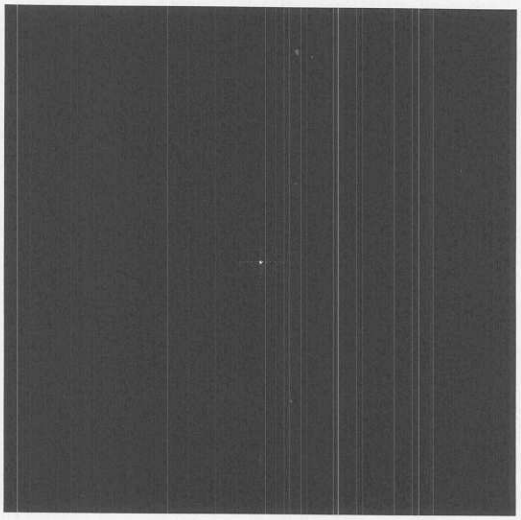

Figure 3.4: Multiple Receiver Ambiguity Function Test Result

We have now accurately detected the single object in the test area without falsely detecting the presence of additional objects. In essence, the multiple receive aperture SAR model has been able to accurately (or unambiguously) map the entire test image area.

Having illustrated the concepts with the use of the ambiguity function, it is now appropriate to begin simulation of the various test environments designed earlier.

4 RESULTS

4.1 Situation 1

In this situation, the prf is set at 7 kHz whilst the single receive aperture has a length of 25.5 cm in the along-track direction and a height of 37.1 cm in the across-track direction. The receiver response is shown as Figure 4.1. The prf setting is sufficient to eliminate range ambiguities, but not doppler ambiguities. The aperture size settings result in a wide swath that illuminates the entire input image area. But, the broad illumination beamwidth now detects points of ambiguity in the doppler direction. This is why we observe repetitions of the input image in the along-track direction. The result is an image that possesses wide swath but also high ambiguity in the along-track direction.

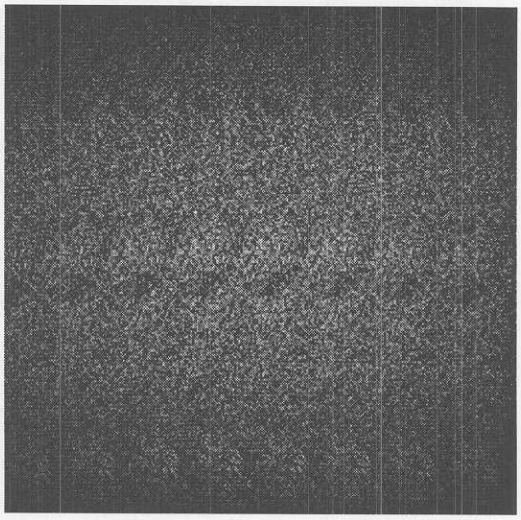

Figure 4.1: Radar Receiver Response for Situation 1

4.2 Situation 2

The poor observation in Figure 4.1 is a result of the wide beamwidth highlighting areas of ambiguity in doppler. We now attempt to alter this beamwidth to lower ambiguity. Thus the prf here is maintained at 7 kHz. To counter the effects of ambiguity in the along-track direction, the along-track aperture length of the single receiver will now be made nine times larger than the original value of 25.5 cm. The across track aperture height remains at 37.1 cm. In Figure 4.2, we observe a thin illumination area in the doppler direction that is now able to eliminate the ambiguities present in the along-track direction. We now have an unambiguous image with a narrow along-track illumination width.

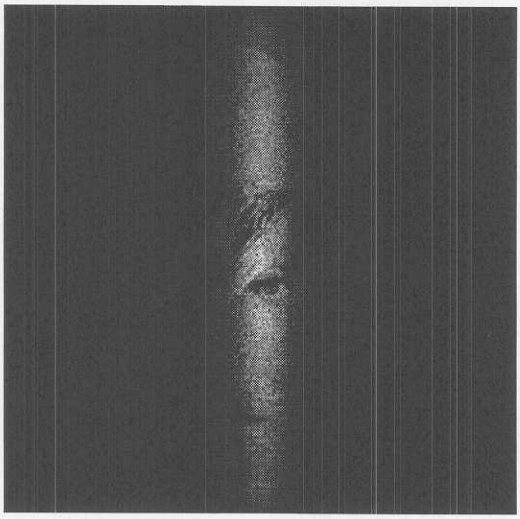

Figure 4.2: Radar Receiver Response for Situation 2

4.3 Situation 3

Figure 4.3 shows the radar receiver response for Situation 3. In this situation, the pulse repetition frequency is now set at a level of 60 kHz. This satisfies the requirement for non-ambiguity in the along-track direction, but does not eliminate ambiguity in the across-track direction. The single receiver aperture size is once again set at 25.5 cm in the along-track direction and 37.1 cm in the across-track direction. This will result in a wide swath width, but our concern here is that this wide swath will now detect ambiguity in the across-track direction. As expected, Figure 4.3 now shows repetitions of the input image area in the across-track direction. The result here is an image with wide swath but also with high ambiguity in the across-track direction.

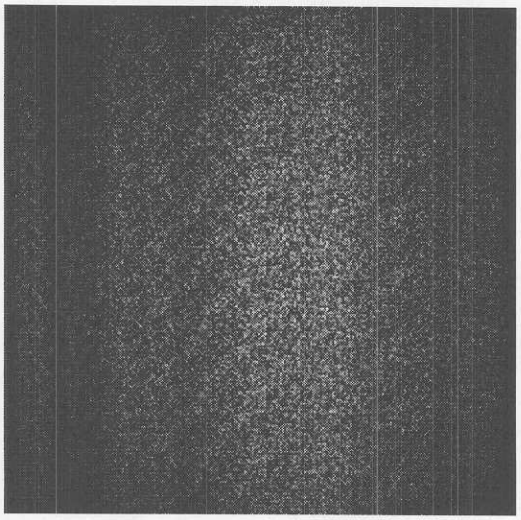

Figure 4.3: Radar Receiver Response for Situation 3

4.4 Situation 4

We observe once again that the poor observation in Figure 4.3 is a result of the wide swath width detecting points of ambiguity in range. A possible solution would be to narrow the swath width. Therefore, in this situation the single receive aperture has an along-track length of 25.5 cm but an across-track height of nine times the original value of 37.1 cm. The pulse repetition frequency is maintained at 60 kHz. Figure 4.4 shows the results obtained for this situation. We observe that there is now a narrow strip in the across-track direction that is able to eliminate all the ambiguities in the direction of range. However, this has come at the expense of narrow coverage in the across-track direction. The result we obtain here is an unambiguous image that now has a narrow swath width.

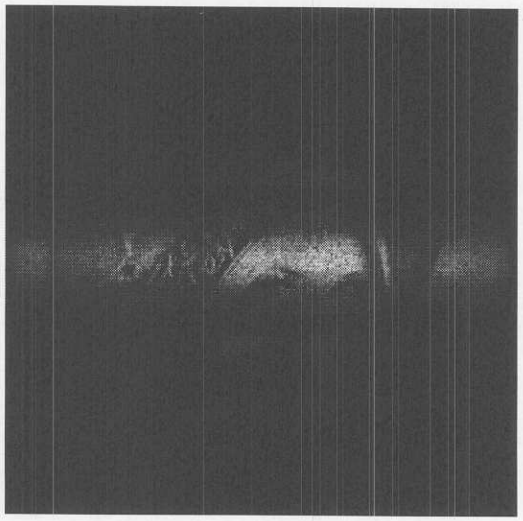

Figure 4.4: Radar Receiver Response for Situation 4

4.5 Situation 5

Next, the pulse repetition frequency was set at a value of 20.5 kHz. This is a factor of three away from either 7 kHz or 60 kHz. The single receive aperture is also set at its original value of 25.5 cm in the along-track direction and 37.1 cm in the across-track direction. With this aperture size, we expect the entire image area to be illuminated. Figure 4.5 shows the results obtained in this situation. With the pulse repetition frequency set at a factor of three away from either extreme, we would thus expect three times less ambiguity in both range and doppler directions. In Figure 4.5, we are able to notice more of the original image than we did in Figures 4.1 and 4.3. We are also able to observe the distinct ambiguous positions in either direction. Thus this situation returns an image with full coverage and moderate ambiguity.

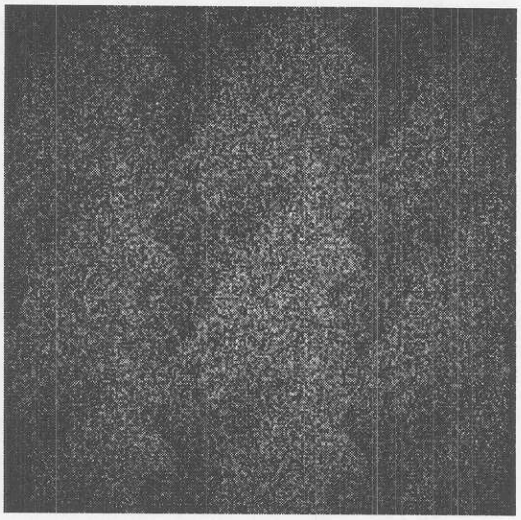

Figure 4.5: Radar Receiver Response for Situation 5

4.6 Situation 6

In the next test situation, the pulse repetition frequency was maintained at the intermediate value of 20.5 kHz. This would again lead us to expect our resultant image to have less ambiguity in both directions. However, in this instance, we alter the value of the along-track aperture length to now read as three times its original value of 25.5 cm. The across-track aperture height remains at 37.1 cm. From this, we would expect a slightly wider illumination beamwidth than we did in Figure 4.2. Figure 4.6 shows the results obtained. We see that by increasing the along-track aperture length, we have eliminated a considerable amount of ambiguity. However, ambiguity remains in the across-track direction due to the fact that a pulse repetition frequency of 20.5 kHz is still too low.

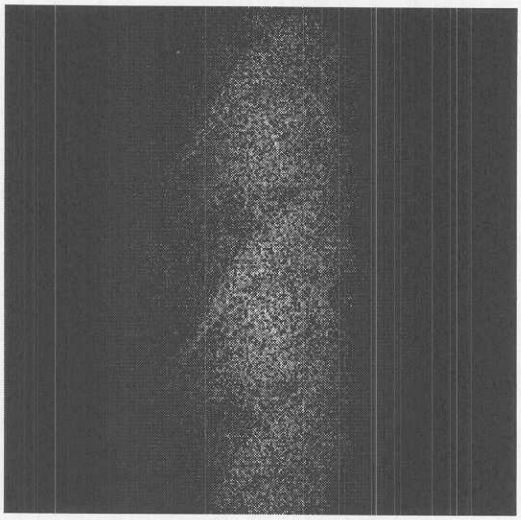

Figure 4.6: Radar Receiver Response for Situation 6

4.7 Situation 7

In Situation 7, it is the across-track aperture height that is now altered to read as three times its original value of 37.1 cm. The along-track aperture length returns to its original value of 25.5 cm. Therefore, we expect a swath width that is slightly wider than that of Figure 4.4. We maintain the pulse repetition frequency at the intermediate value of 20.5 kHz. Once again, this leads us to expect a factor of three reduction in ambiguity. Figure 4.7 shows the results obtained for this situation. As expected, we have eliminated all the ambiguity in the across-track direction by enlarging the across-track aperture height. However, a pulse repetition frequency of 20.5 kHz is not sufficiently high enough to eliminate all the along-track ambiguity within the illumination area. We are left with an ambiguous image that has limited swath coverage.

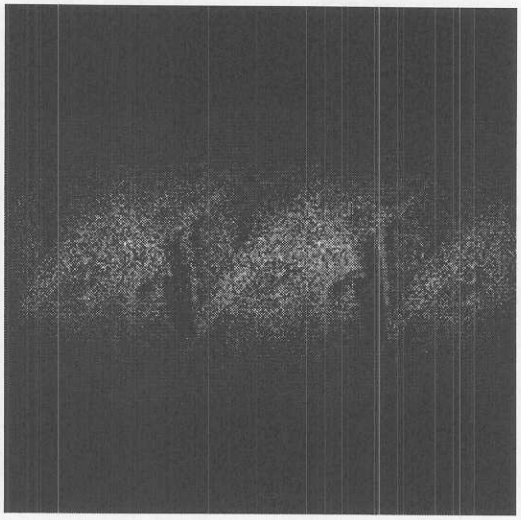

Figure 4.7: Radar Receiver Response for Situation 7

4.8 Situation 8

Here, we aim for some sort of compromise between ambiguity and swath width. We maintain the pulse repetition frequency at the intermediate level of 20.5 kHz. We alter the along-track aperture length to be three times its original value of 25.5 cm and the across-track aperture height to be three times its original value of 37.1 cm. The intermediate pulse repetition frequency will reduce the ambiguity by a factor of three in each direction. In addition, the larger aperture size in both directions will also be able to reduce ambiguity by a further factor of three in both directions. We would thus expect an unambiguous image here. Figure 4.8 shows the results obtained in this situation. We observe that our prediction was true. But, this has now come at the expense of a narrow swath width and a narrow illumination beamwidth.

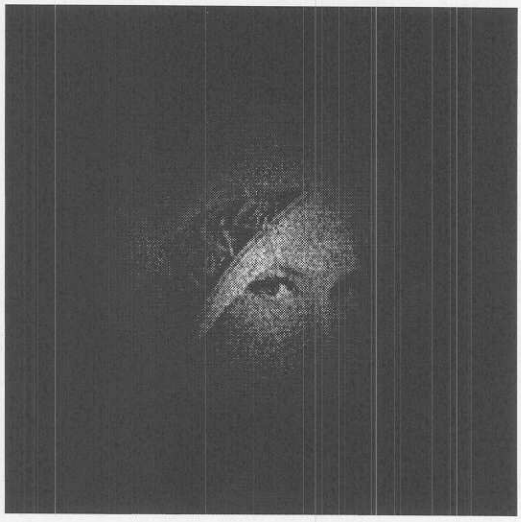

Figure 4.8: Radar Receiver Response for Situation 8

4.9 Situation 9

This situation marks the transition to a multiple receive aperture SAR environment. From hereon, all receive apertures have a fixed length of 25.5 cm in the along-track direction and height of 37.1 cm in the across-track direction. Here, we design three receive apertures lined up in the along-track direction. The pulse repetition frequency is maintained at the intermediate value of 20.5 kHz. We see a marked improvement now in the performance as compared to Figure 4.6. The additional apertures in the along-track direction have allowed for a wider illumination beamwidth in Figure 4.9 without any further increase in ambiguity from Figure 4.6. This was previously unachievable in the single receive aperture environment. However, whilst this is an improvement over the single aperture environment, the existing across-track ambiguity is undesirable.

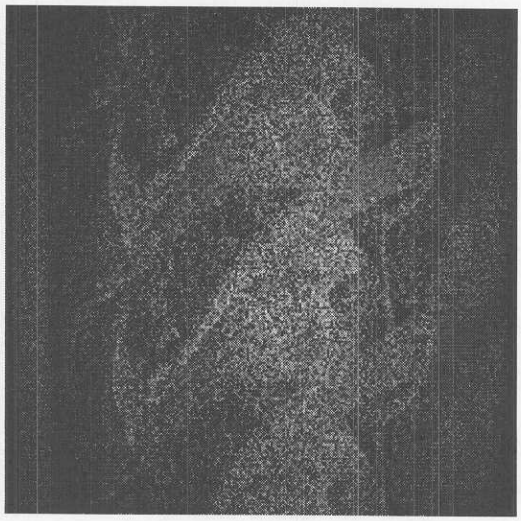

Figure 4.9: Radar Receiver Response for Situation 9

4.10 Situation 10

In this situation, the pulse repetition frequency is maintained at 20.5 kHz. The three receive aperture design is also maintained, but these apertures are now laid out in the across-track direction. The result for this situation is shown as Figure 4.10. Here, we also notice a marked improvement in performance as compared to Figure 4.7. Whilst the ambiguity in the along-track direction remains the same, the three receive apertures in the across-track direction have allowed for a wider swath width to be present in the image. This, once again, was an unachievable goal in the single receive aperture environment. However, the remaining ambiguity is undesirable and clearly indicates that three apertures is an insufficient number to return an unambiguous image.

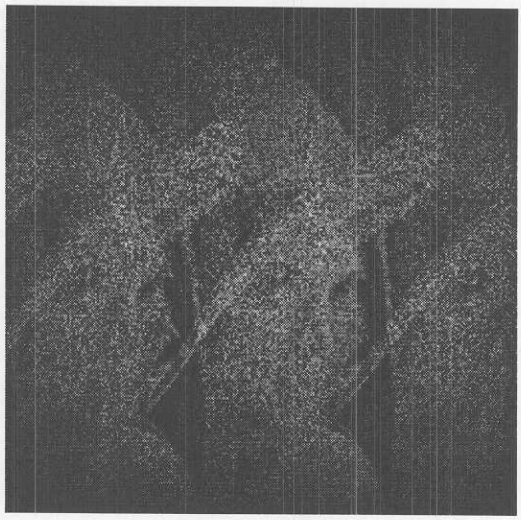

Figure 4.10: Radar Receiver Response for Situation 10

4.11 Situation 11

This situation marks the beginning of the nine receive aperture design phase. Here, we start once again by returning to a prf of 7 kHz that will eliminate range ambiguities but not ambiguities in the doppler direction. We also design the multiple receive aperture unit such that there are three apertures in the across-track direction and three in the along-track direction. With three apertures present, we expect the ambiguity in the along-track direction to be reduced by a factor of three. The result is a significant improvement over Figure 4.1. However, because the apertures are not oriented in the right manner, there remains ambiguity in the along-track direction. With a low prf, all ambiguity in the across-track direction is eliminated and it is pointless to place additional apertures in the direction of range.

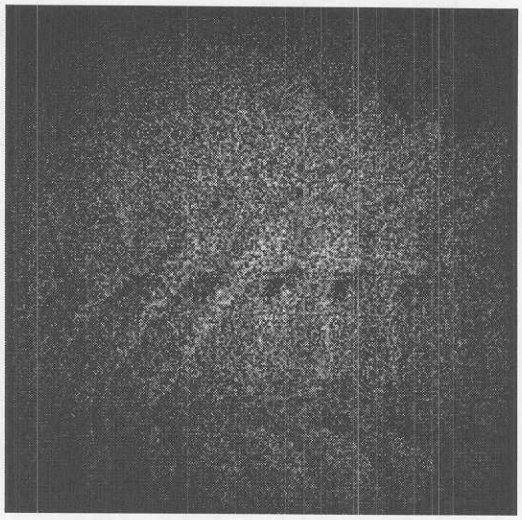

Figure 4.11: Radar Receiver Response for Situation 11

4.12 Situation 12

In this situation, we work to improve the result achieved in Figure 4.11. From the results achieved in Situation 11, it is clear that with a pulse repetition frequency of 7 kHz, there is no longer a need for additional apertures in the across-track direction. A more appropriate design would be to maintain the nine aperture design but orientate the apertures in such a manner that there are nine apertures in the along-track direction. With a low prf, the along-track direction is where ambiguity exists and, thus, needs to be removed. Finally, we have arrived at a satisfying result. We now have a resultant unambiguous image that possesses high resolution and wide swath. A multiple receive aperture SAR environment coupled with proper orientation of apertures has allowed us to achieve this.

Figure 4.12: Radar Receiver Response for Situation 12

4.13 Situation 13

We now refocus our attention on a pulse repetition frequency of 60 kHz. This value will eliminate ambiguity in the along-track direction but not in the across-track direction. We return to our nine aperture receiver design with three apertures aligned in the across-track direction and three aligned in the along-track direction. We can now predict that this may not be the best receiver orientation to give us optimum performance. Although the multiple receivers have provided us with a wide swath, there exists ambiguity in the across-track direction due to incorrect receiver orientation. It is pointless here to add receivers in the along-track direction when our choice of prf will already ensure that no ambiguity is present in the doppler direction. The three receive apertures in the across-track direction are only sufficient to reduce ambiguity by a factor of three.

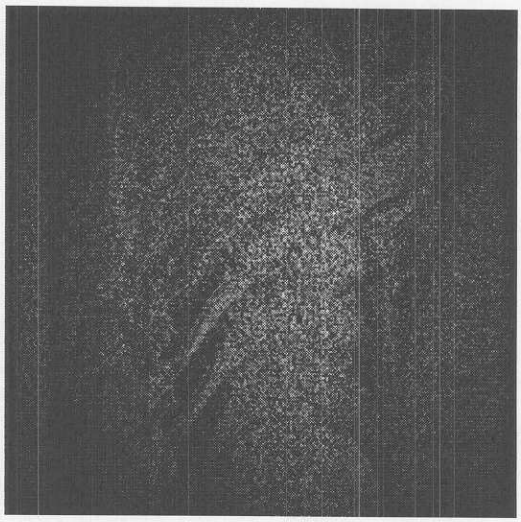

Figure 4.13: Radar Receiver Response for Situation 13

4.14 Situation 14

We now attempt to improve upon our results achieved in Figure 4.13. It is clear that our receiver design in Situation 13 was incorrect. A choice of 60 kHz as the pulse repetition frequency effectively eliminates doppler ambiguities. There is no longer a need to place additional receivers in the along-track direction. Rather, it would seem that the nine receivers should all be placed in the across-track direction. This would provide the desired ambiguity reduction factor of nine in the across-track direction. Figure 4.14 shows the another extremely satisfying result obtained. We have once again managed to obtain an unambiguous image that possesses high resolution and wide swath width. The result obtained in Figure 4.14 is identical to that obtained in Figure 4.12. This point of note will be extremely useful once the results for the following section are finally obtained.

Figure 4.14: Radar Receiver Response for Situation 14

4.15 Situation 15

Finally, we return to a prf of 20.5 kHz. With experience from previous situations, we know that this choice of pulse repetition frequency reduces ambiguity in both along-track and across-track directions by a factor of three. We are now able to predict that our multiple receive aperture design must reduce the ambiguity by a further factor of three before we are able to obtain an unambiguous image. Thus, there must be three apertures in the across-track direction and three apertures in the along-track direction of the receiver. We have obtained an unambiguous image that has high resolution and wide swath. Also, whilst they were all generated based on different pulse repetition frequencies, Figures 4.12, 4.14, and 4.15 are identical. The multiple receive aperture SAR environment has relinquished the dependence of its receiver response on the prf.

Figure 4.15: Radar Receiver Response for Situation 15

4.16 Summary of Results

The results obtained are extremely encouraging. From Situations 1 through 8, we have illustrated the current limitation in conventional SAR data processing. Through careful adjustment of design parameters, we may obtain a high resolution, unambiguous image at the expense of a narrow swath width. In addition, we may also obtain a wide swath, moderate resolution image that possesses ambiguity. However, the conventional single receive aperture SAR will not allow us to obtain a wide swath, high resolution, and unambiguous image at the same time.

Situations 9 and 10 represent the initial transition to the multiple receive aperture SAR environment. From the previous chapter, we know that the system was designed to provide an ambiguity factor of nine. The three receive aperture SAR model environment was created to show a significant, albeit insufficient, performance improvement. We have obtained a wide swath image but reduced the ambiguity by only a factor of three. There clearly is room for improvement.

Situations 11 through 15 show the final results with the nine receive aperture SAR model. We have seen that, regardless of the pulse repetition frequency, we are able to adjust the orientation of the receivers in such a manner to obtain a wide swath, high resolution, and unambiguous image simultaneously. This was the original aim of this project and it is satisfying to note that our theory has been physically proven.

We reiterate here that there may very well be more than nine receive apertures in a particular design. From the previous chapter, we understand that this simulation environment was designed to produce unambiguous images when a total of nine receive apertures are used. The three receive aperture environment was introduced to show an intermediate performance improvement over the single receive aperture scenario. Whilst using nine receive apertures in our design situation is sufficient to produce unambiguous images, selection of a number that is larger than nine will result in a larger collection of independent samples. The presence of these additional receive apertures will consequently cause a larger amount of energy backscatter to be collected and, therefore, lead to an increase in the SNR of the radar system.

5 CONCLUSION AND FUTURE WORK

5.1 Conclusion

This project has documented in detail the performance benefits of a multiple receiver Synthetic Aperture Radar system in contrast to a single receiver one. The workings of a SAR in both a single and multiple receive aperture environment have been illustrated through the use of both mathematics and graphics.

Numerical examples have been provided as a proof of the current limitations of the present system. The same example (for both a fully focused and partially focused aperture) was executed after the proposed solution was documented to show mathematically the performance improvement that a multiple channel SAR has over a single channel one.

A design and simulation environment was developed to test the new SAR model. The model was developed in a manner such that only minor changes were necessary for conversion from a single receive aperture environment to a multiple receive aperture one. The single receive aperture case illustrated all the present problems. For the multiple receive aperture case, situations involving both three and nine receive apertures were tested to show some variation in the performance improvement.

In particular, it has been shown that the single receiver SAR environment constantly faces a tradeoff involving ambiguity, resolution, and swath width. A

high pulse repetition frequency is necessary in order to eliminate ambiguity in the along-track direction. However, we also require a low pulse repetition frequency to eliminate ambiguity in the across-track direction. Compensation to this ambiguity may be made in either direction by reducing the illumination area. However, this later results in a narrow swath width. As a result, it is impossible (in the single receiver SAR environment) to complete eliminate ambiguity in both the along-tack and across-track directions whilst maintaining wide swath width and high resolution.

A Synthetic Aperture Radar simulator was constructed using the C programming language. This simulator was first employed in a single receive element environment. Several test situations were developed and then simulated to generate output images that physically illustrate the difficulties currently present in the single receive aperture SAR environment.

The multiple receiver SAR environment has alleviated this problem because the restriction imposed by the time-bandwidth product is now lifted. We are now able to obtain a sufficient number of independent samples in order to generate an unambiguous result. This model has now relieved the dependence of the receiver response on the pulse repetition frequency. An unambiguous, wide swath, high resolution image may be now generated independent of the choice of pulse repetition frequency.

We presently only need to add a minimum number of receivers that will allow us to obtain data samples equal to the number of pixels in the imaged area, thereby eliminating ambiguity. The inclusion of additional receivers that generate samples in excess of the total number of image pixels will result in the collection of a larger amount of energy backscatter. This will in turn result in an increase in the SNR of the system, which is a desirable feature. Alternatively, we may also wish to maintain the SNR at a pre-defined level and subsequently lower the power level of the radar system.

The SAR simulator developed earlier was next modified to operate in a multiple receive element environment. Once again, several test situations were developed and simulated to produce output images that reflect a significant improvement in performance over the single receiver environment. Specifically, it was proven that when multiple receivers are employed in a SAR, it is possible to generate a high resolution, wide swath, and unambiguous SAR image.

5.2 Future Work

Moving target indication (MTI) is another area of Synthetic Aperture Radar data processing where there is currently a considerable amount of ongoing research. In conventional SAR imaging, it is the ground - and any stationary object on it - that is the target. However, the doppler shift that a moving target generates now competes with the SAR's doppler shift generation. It is this

phenomenon that makes moving targets difficult to resolve in SAR imaging. Whilst there have been new methods such as reflectivity displacement [17] and radial velocity band filtering [18] that have been offered as possible partial solutions to this problem, there undoubtedly remains a great deal of research work to be done in the area of SAR moving target indication.

It was because of this current demand that, in the course of software development for the multiple receive element SAR simulator, it was ensured that functionality for future testing of this model on moving targets was also included. In essence, a velocity vector that defines each point in the imaged area has been included as part of the model. As this project primarily focused on obtaining wide swath, high resolution, and unambiguous images from objects that were stationary and ground-based, this velocity vector was simply defined as null.

Furthermore, this velocity vector has been designed with three dimensional **x**, **y**, and **z** coordinates. This has allowed for the possibility that an object may be moving on the ground, i.e. the **x-y** plane, or it may be heading away from the ground and in the air, i.e. the **x-y-z** space. Consequently, the position of the object at any time t may now lie on the ground (the **x-y** plane) if it is stationary or has a two dimensional ground velocity vector. Alternatively, the position vector may also lie in the air (the **x-y-z** space) if it now has a three dimensional airborne velocity vector. For this reason, the position vector of the

object at any time t has also been designed with three dimensional **x**, **y**, and **z** coordinates.

Therefore this model has been consciously designed to be suitable for radar signal processing research projects involving ground moving target indication (GMTI) as well as airborne moving target indication (AMTI). With a few straightforward modifications and the simple introduction of a ground or an airborne velocity, the multiple receive element SAR simulator constructed may easily be employed in a variety of test situations for future research projects on SAR-MTI.

REFERENCES

[1] A. Currie, "Synthetic Aperture Radar", *Electronics and Communications Engineering Journal*, August 1991, pp. 159-170.

[2] A. Currie, & M.A. Brown, "Wide Swath SAR", *IEE Proceedings – F*, Vol. 139, No. 2, April 1992, pp. 122-135.

[3] A. Currie, & C.D. Hall, "A Synthetic Aperture Radar Technique for the Simultaneous Provision of High Resolution Wide Swath Coverage", *Proceedings Military Microwaves '90*, Microwaves Exhibitions and Publishers Ltd., July 1990, pp. 539-544.

[4] H.D. Griffiths, & P. Mancini, "Ambiguity Suppression in SARs using Adaptive Array Techniques", *Proceedings of IGARSS 1991 Symposium*, 1991, pp. 1015-1018.

[5] S. Barbarossa, & A. Farina, "Space-Time-Frequency Processing of Synthetic Aperture Radar Signals", *IEEE Transactions on Aerospace and Electronic Systems*, Vol. 30, No. 2, April 1994, pp. 341-358.

[6] H. Steyskal, "Digital Beamforming Antennas: An Introduction", *Microwave Journal*, January 1987, pp. 107-124.

[7] H. Steyskal, & J.F. Rose, "Digital Beamforming for Radar Systems", *Microwave Journal*, January 1989, pp. 121-136.

[8] J. Stiles, "Wide Swath, High Resolution, Low Ambiguity SAR using Digital Beamforming Arrays", *AFOSR Summer Research Extension Proposal*, October 1996.

[9] F.T. Ulaby, A.K. Fung, & R.K. Moore, *Microwave Remote Sensing, Active and Passive, Vol. 2: Radar Remote Sensing and Surface Scattering and Emission Theory*, Artech House Inc., 1982.

[10] N. Levanon, *Radar Principles*, John Wiley & Sons Inc., 1988.

[11] W.L. Stutzman, & G.A. Thiele, *Antenna Theory and Design*, John Wiley & Sons Inc., 1981.

[12] S. Haykin, *Communication Systems*, John Wiley & Sons Inc., 1994.

[13] L. Rade, B. Westergren, *Mathematics Handbook for Science and Engineering*, Birkhauser, 1995.

[14] M.I. Skolnik, *Radar Handbook*, McGraw Hill Inc., 1990.

[15] J.R. Hanly, E.B. Koffman, & J.C. Horvath, *C Program Design for Engineers*, Addison Wesley, 1995.

[16] H.M. Deitel, & P.J. Deitel, *C How to Program*, Prentice Hall Inc., 1994.

[17] J.R. Moreira, & W. Keydel, "A New MTI-SAR Approach using the Reflectivity Displacement Method", *IEEE Transactions on Geoscience and Remote Sensing*, Vol. 33, No. 5, September 1995, pp. 1238-1244.

[18] A. Freeman, & A. Currie, "Synthetic Aperture Radar (SAR) Images of Moving Targets", *The GEC Journal of Research*, Vol. 5, No. 2, 1987, pp.106-115.

APPENDIX A DERIVATION OF RADAR ANTENNA COORDINATE AXES

For convenience, Figure 2.2 depicting the radar antenna coordinate geometry is reproduced here once again.

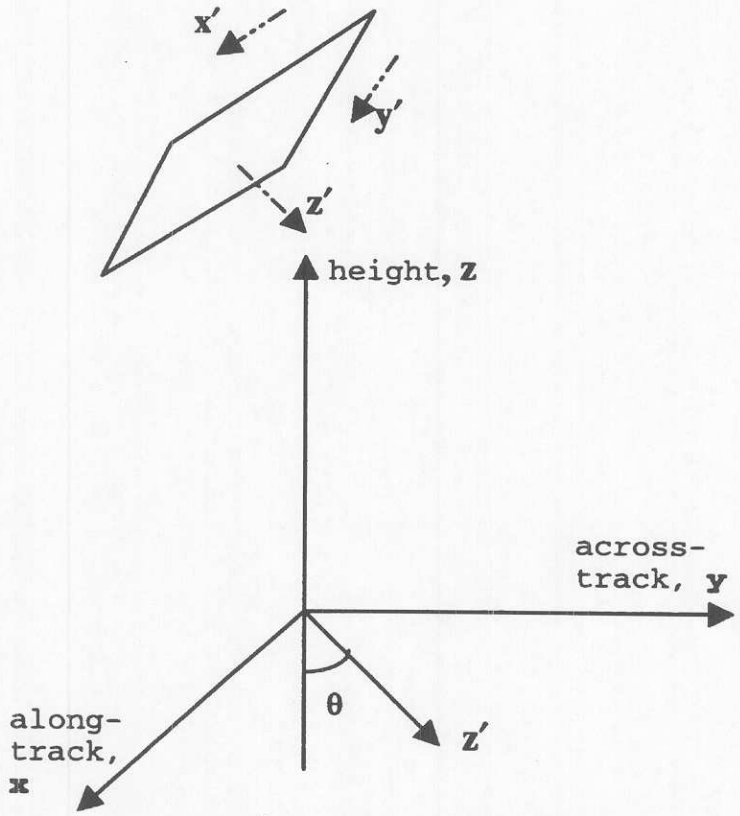

Figure 2.2: Radar Antenna Coordinate Geometry

Since the radar antenna is essentially rotated about the **x** axis, the derivation of the relationship between **x′** and the conventional axes is trivial:

$$\hat{x}' = \hat{x}\,. \qquad \text{(A.1)}$$

A significant portion of the remaining derivation involves the use of the dot product. By definition,

$$\vec{a} \bullet \vec{b} = |\vec{a}||\vec{b}|\cos\phi, \tag{A.2}$$

where ϕ is the angle between vectors **a** and **b**.

Keeping in mind that θ is the angle between the **z** and **z′** directions, we can now see that

$$\hat{z}' \bullet \hat{z} = \cos(\pi - \theta), \tag{A.3}$$

and also that

$$\hat{z}' \bullet \hat{y} = \sin\left[\frac{\pi}{2} - \theta\right]. \tag{A.4}$$

From trigonometry [13], we know that

$$\cos(\pi - \theta) = -\cos\theta, \tag{A.5}$$

and also that

$$\sin\left[\frac{\pi}{2} - \theta\right] = \sin\theta. \tag{A.6}$$

Therefore, we can now use equation (A.5) and simplify equation (A.3) to read as

$$\hat{z}' \bullet \hat{z} = -\cos\theta. \tag{A.7}$$

Similarly, we can now use equation (A.6) and simplify equation (A.4) to read as

$$\hat{z}' \bullet \hat{y} = \sin\theta \tag{A.8}$$

From equations (A.7) and (A.8), we can collectively deduce now that

$$\hat{z}' = (\sin\theta)\hat{y} - (\cos\theta)\hat{z}. \tag{A.9}$$

Similarly, we are now also able to make the following statements:

$$\hat{z} \bullet \hat{y}' = \cos\left[\frac{\pi}{2} + \theta\right], \tag{A.10}$$

and

$$\hat{y} \bullet \hat{y}' = \cos(\pi - \theta). \tag{A.11}$$

From trigonometry [13], we also know that

$$\cos\left[\frac{\pi}{2} + \theta\right] = -\sin\theta. \tag{A.12}$$

Therefore, we are now in a position to use equation (A.12) to simplify equation (A.10) to be

$$\hat{z} \bullet \hat{y}' = -\sin\theta. \tag{A.13}$$

We can also use equation (A.5) to simplify equation (A.11) to now read as

$$\hat{y} \bullet \hat{y}' = -\cos\theta. \tag{A.14}$$

From equations (A.13) and (A.14), we can now further deduce that

$$\hat{y}' = (-\cos\theta)\hat{y} - (\sin\theta)\hat{z}. \tag{A.15}$$

Equations (A.1), (A.9) and (A.15) now provide us the relationships between the radar antenna coordinate axes and the conventional object coordinate axes.

UNAMBIGUOUS, HIGH RESOLUTION, AND WIDE SWATH SYNTHETIC APERTURE RADAR IMAGING

by

DEVINDRAN RAJAKRISHNA
B.S.(Honors), Electrical Engineering
The University of Iowa, 1996

Submitted to the Department of Electrical Engineering and Computer Science and
the Faculty of the Graduate School of the University of Kansas
in partial fulfillment of the requirements for the degree of
Master of Science in Electrical Engineering

Thesis Committee:

_____

Chairperson

_____

_____

Date of Defense: _____

For Sujatha, who has brought such joy into my life.

ACKNOWLEDGMENTS

I am indeed fortunate to have had three competent and caring faculty members on my committee. Prof. Jim Stiles has been an excellent advisor whose confidence and enthusiasm helped me remain focused throughout the project. Prof. John Gauch could take a single look at several lines of my code and tell me immediately where I was going wrong. Prof. Chris Allen was my first supervisor at the University of Kansas and has always found extra time for me.

Fadi Wahhab spent many of his evenings assisting me with the debugging of the computer code and helped me through the toughest part of the project. Paola Parra is a true gem of a person whose lovely smile and affection never failed to brighten my day. Beng Beh and Sudha Krishnaswami also tirelessly helped in the proofreading of this manuscript.

Reza and Tammy Hosseinmostafa, and Barbara Hunn have been such wonderful friends. They are very special to me.

I extend my appreciation to all the people who have made my time at RSL so enjoyable. In particular, I'd like to thank Donnis Graham, Pannirselvam Kanagaratnam, Mario Pavlovic, and Deb Chatterjee.

Most importantly, I send my heartfelt thanks to my mother Lohambal, brother Pravin, sister Marleni, and brother-in-law Sascha for all their continued love and support. Also, this could not have been possible without the invaluable guidance of my late father, Rajakrishna, during my formative years.